Supporting Information

Promoting water splitting on arrayed molybdenum carbide nanosheets with electronic modulation

Jinxiang Diao‡, Xiaolin Li‡, Shuya Wang, Zejun Zhao, Weitao Wang, Kai Chen, Tingting Chao, Yong Yang**

Experiment Section

Preparation of N-Mo_2C: All the chemical reagents were of analytical grade and used without further purification. Two piece of Ni foam (2 cm×1.5 cm) were cleaned ultrasonically in 2 M HCl for 30 min and washed with water and absolute alcohol for 3 times. Then 0.6 g $(NH_4)_6Mo_7O_{24}.4H_2O$ was dissolved in 30 mL of water, and 880 μL ethylenediamine (EDA) were dissolved in 30 mL of distilled water under continuities stirring. The feed percentage of ethylenediamine (EDA) was 440 μL and 1320 μL respectively. Then, the pH value of solution was adjusted to 4-5 using 2 M HCl until the white precipitate appears. The mixture solution was transferred into a 50 mL Teflon-lined stainless steel autoclave, and Ni foam was placed upright in the autoclave. The autoclave was heated to 150 °C in an electric oven and maintained for 12 h. After that Ni foam with precursor was cleaned with ethanol and deionized water for several times before being fully dried in a vacuum oven at 60 °C for overnight. Then the Ni foam with precursor was reduced at 450 °C for 2 h in H_2/Ar (v/v, 5/95) atmosphere to achieved sample. According to their XPS result, they are denoted as N-Mo_2C-1/NF (2.25 awt%), N-Mo_2C/NF (6.78 awt%) and N-Mo_2C-3/NF (10.25 awt%). Further 20 wt% Pt/C, IrO_2 and Ni foam was tested for comparison.

Preparation of Mo_2C and Mo_2N : MoO_3-EDA precursor was synthesized via the previously described method.[1] 500 mg MoO_3-EDA was transferred into a tube furnace and heated to the temperature of 650 °C at a heating rate of 5 °C min^{-1} and holding for 3 h under the atmosphere of 5 vol % H_2/Ar. After naturally cooling down, the Mo_2C was obtained. Under the NH_3 atmosphere, the Mo_2N were obtained.

Structural Characterization: Powder X-ray diffraction (XRD) of all samples was performed on a Bruker D8 ADVANCE diffractometer using Cu Kα radiation. The morphology and nanostructure of N-Mo_2C was observed by high-resolution field emission SEM (JEOL JSM-6390A) and transmission electron microscope (TEM, G^2 F20 S-TWIN), aberration-corrected HAADF-STEM instrument (Themis Z, FEI) at 300 kV together with a SEM (SU8220, Hitachi) at 15 kV. The specific surface areas and the distribution of pore size were tested by N_2 adsorption at 77 K, using instrument Micromeritics Tristar-3020. The chemical state of the elements in N-Mo_2C was measured by X-ray photoelectron spectroscopy (XPS) on a Thermo Fisher Escalab 250Xi. X-ray monochromator was microfocused Al Kα radiation. Raman spectra was obtained from Renishaw Ramanscope. X-ray absorption fine structure (XAFS) spectra at the W K-edge were recorded at the 1W1B station of Beijing Synchrotron Radiation Facility (BSRF), China.

Electrochemical Measurements: All the electrochemical measurements were carried out were performed on a CHI 700E electrochemical workstation (CH Instruments, China). For HER and OER, the Ni supported N-Mo_2C was directly used as the working electrodes with testing area of 0.25 cm^2. A saturated Ag/AgCl and a graphite rod was used as the reference electrode and counter electrode. Electrochemical impedance spectroscopy (EIS) was carried out in frequency range of 100 kHz-0.1Hz under a potential of 100 mV in KOH solution. In addition, the double layer capacitance (C_{dl}) was evaluated from the relationship of the capacitive current ($\Delta j = j_{anodic} - j_{cathodic}$) vs. potential scan rates, which was considered to be proportional to electrochemical active surface area (ECSA).[2]

The overall water splitting is performed in a two-electrode system. The long-term potential vs. time plots were obtained under a current density of 10 $mA \cdot cm^{-2}$ for 24 h.

IR-correction: Unless stated otherwise, all polarization curves measured in a threeelectrode configuration are *i*R-corrected. The correction was done according to the following equation:

$$E_{corr} = E_{mea} - iR_c$$

Where E_{corr} is *i*R-corrected potential, E_{mea} experimentally measured potential, and R_c is the compensated resistance[3].

DFT theoretical calculations: The present first principle DFT calculations are performed with the projector augmented wave (PAW) method.[4] The gradient approximation (GGA) with Perdew-Burke-Ernzerhof (PBE) functional was used for exchange-functional. The cut-off energy of the plane-wave basis is set at 400 eV. The vacuum spacing in a direction perpendicular to the plane of the catalyst is at least 10 Å. The Brillouin zone integration is performed using 3×3×1 Monkhorst and Pack k-point sampling for a primitive cell. All the atoms in these structures were fully relaxed to using the conjugated gradient method until a convergence criterion of 10^{-6} eV for energy and 0.03 eV/Å for force.

The OER is considered, as below:

$$*+H_2O(l) \rightarrow OH*+H^+ + e^- \quad (1)$$

$$OH*+H_2O(l) \rightarrow O*+H^+ + e^- \quad (2)$$

$$O*+H_2O(l) \rightarrow OOH*+H^+ + e^- \quad (3)$$

$$OOH* \rightarrow O_2(g)+H^+ + e^- \quad (4)$$

where * is an adsorption site on catalysts. l and g is liquid and gas phases, respectively.

Therefore, the ΔG for each step can be calculated by:

$$\Delta G_1 = G(OH*) + G(H^+ + e^-) - G(H_2O) - G(*)$$

$$= \{\Delta G_{OH*} + G(*) + [G(H_2O - 1/2G(H_2)]\} + 1/2G(H_2) - G(H_2O) - G(*)$$

$$= \Delta G_{OH*}$$

$$\Delta G_2 = G(O*) + G(H + e^-) - G(OH*)$$

$$= \{\Delta GO* + G(*) + [G(H_2O) - G(H_2)]\} + 1/2G(H_2) - \{\Delta GOH* + G(*) + [G(H_2O) - 1/2G(H_2)]\}$$

$$= \Delta G_{O*} - \Delta G_{OH*}$$

$$\Delta G_3 = G(OOH*) + G(H^+ + e^-) - G(O*) - G(H_2O)$$

$$= \{\Delta G_{OOH*} + G(*) + [2G(H_2O) - 3/2G(H_2)]\} + 1/2G(H_2) - \{\Delta G_{O*} + G(*) + [G(H_2O) - G(H_2)]\} - G(H_2O)$$

$$= \Delta G_{OOH*} - \Delta G_{O*}$$

$$\Delta G_4 = G(O_2) + G(H + e^-) - G(OOH*)$$

$= \{4.92 + 2G(H_2O) - 2G(H_2)\} + 1/2G(H_2) - \{\square GOOH^* + G(*) + [2G(H_2O) - 3/2G(H_2)]\}$
$= 4.92 - \square G_{OOH^*}$

Then the free energies can be obtained by including the zero point energy (ZPE) and the entropy (S) corrections in equation $G = Eads - E_{ZPE} - TS$. The E_{ZPE} could be obtained from the calculation of vibrational frequencies for the adsorbed species.

Finally, Chemisorption energies of atomic hydrogen were calculated relative to H_2 (g) by: $E = E(surface + nH) - E(surface) - \frac{1}{2}E(H_2)$.

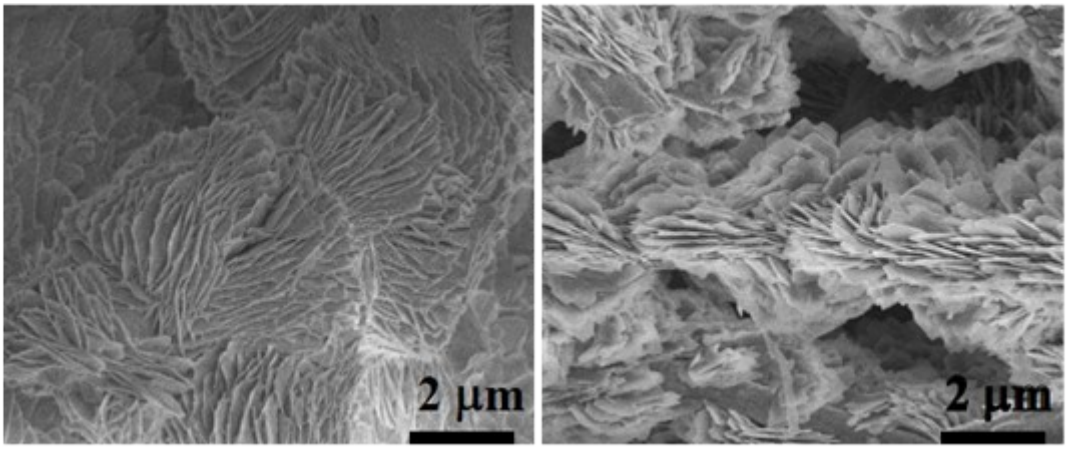

Figure S1. SEM of pure Mo_2C/NF and Mo_2N/NF.

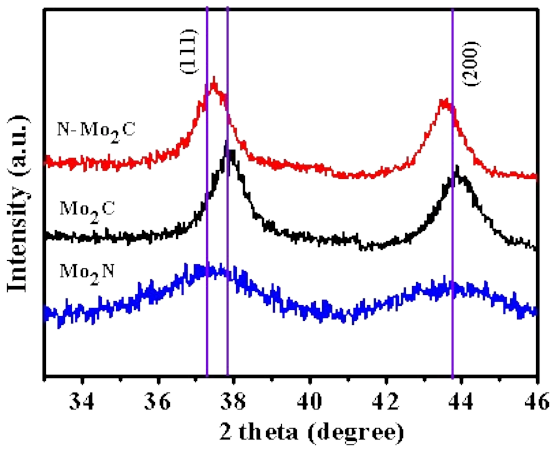

Figure S2. XRD of the pure N-Mo_2C, Mo_2C and Mo_2N (zoom-in region between 33° and 46°).

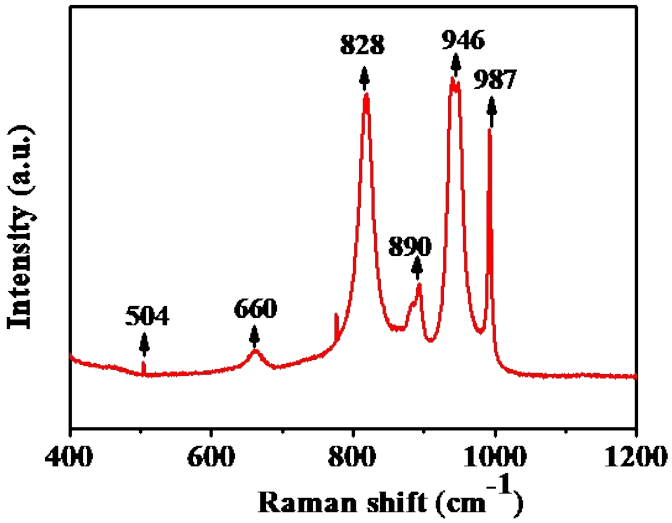

Figure S3. Raman spectra of N-Mo_2C/NF.

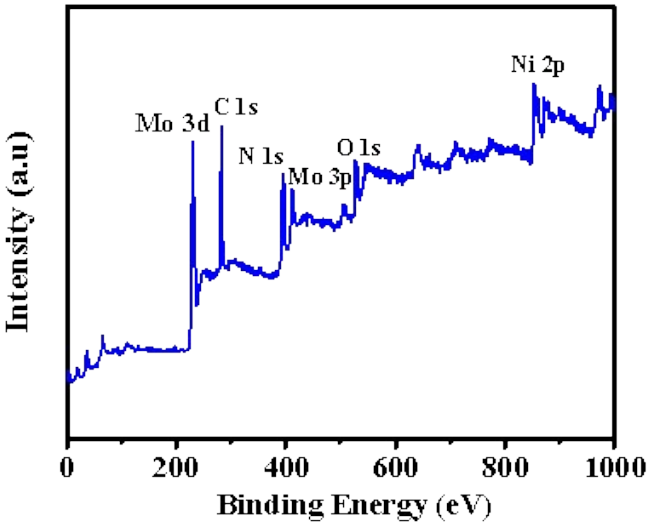

Figure S4. Full spectrum X-ray photoelectron spectroscopy (XPS) spectra of N-Mo_2C/NF

Table S1. XPS fitting parameters for Mo 3d spectrum of N-Mo_2C/NF, Mo_2C/NF, and Mo_2N/NF

Catalyst	$Mo3d_{5/2}$ (eV)	FWHM	The peak area ratio (%)	$Mo3d_{3/2}$ (eV)	FWHM	The peak area ratio (%)	Peak shape
N-Mo_2C/NF	229.5	1.65	60	232.7	1.65	40	GL
Mo_2C/NF	229.0	1.70	60	232.2	1.70	40	GL
Mo_2N/NF	230.0	1.93	60	233.1	1.93	40	GL

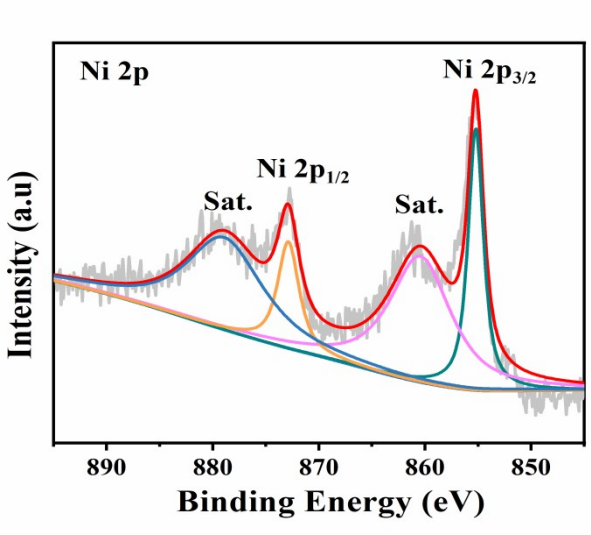

Figure S5. XPS spectra of Ni 2p for N-Mo_2C/NF Nanosheets

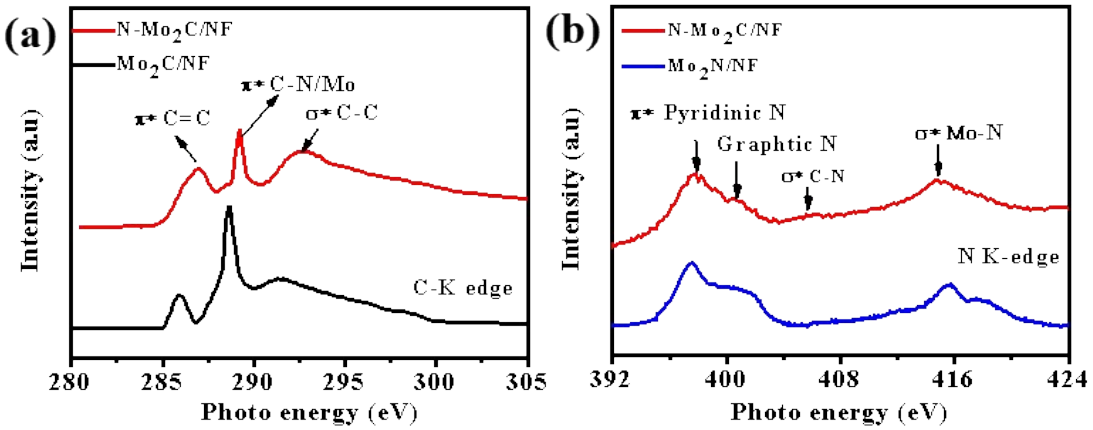

Figure S6. (a) C K-edge XANES spectra of the N-Mo_2C/NF and Mo_2C/NF. (b) N K-edge XANES spectra of the N-Mo_2C/NF and Mo_2N/NF.

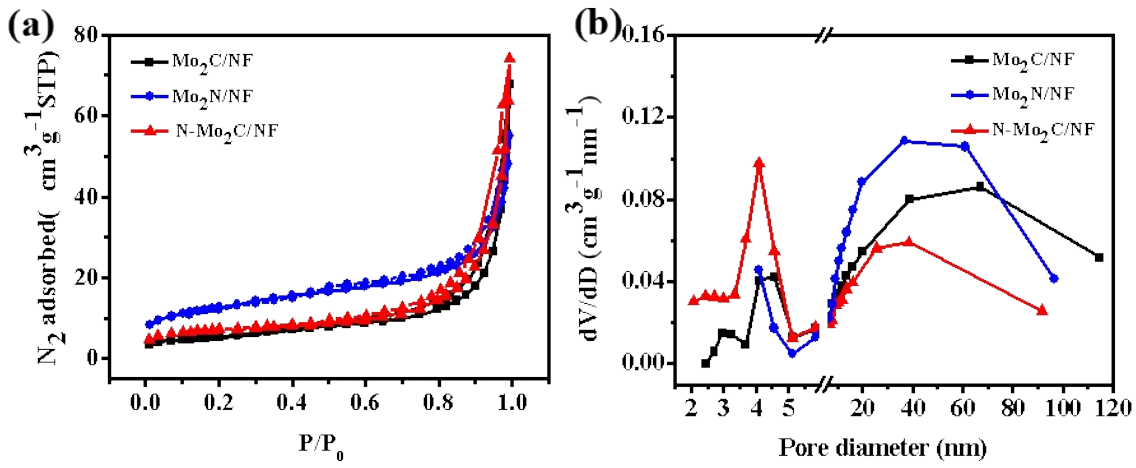

Figure S7. (a) N_2 adsorption/desorption isotherms and of Mo_2C/NF, Mo_2N/NF and N-Mo_2C/NF. (b) corresponding pore distribution of Mo_2C/NF, Mo_2N/NF and N-Mo_2C/NF.

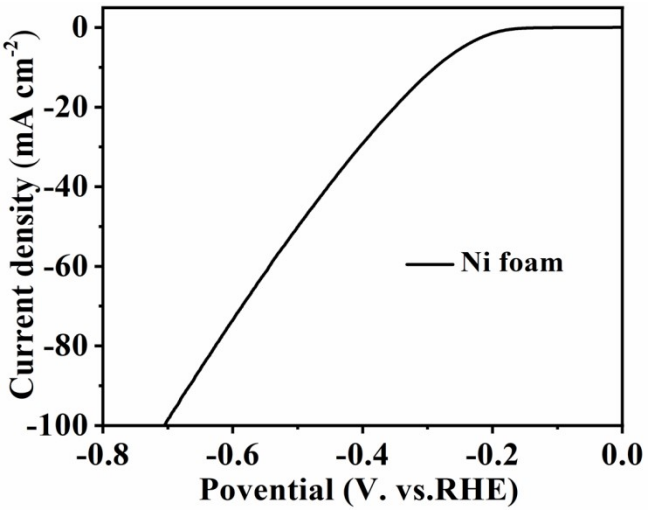

Figure S8. Polarzation curves of Ni foam in 1.0 M KOH at scan of 5 mV s^{-1} for HER.

Table S2. HER performances of N-Mo_2C/NF and other reported electrocatalysts.

Catalyst	**Media**	**(mV) at j=10mAcm^{-2}**	**Reference**
N-Mo_2C/NF	1.0 M KOH	83.9	This work
Ni/TMC	1.0 M KOH	128	*Adv. Energy Mater.* **2020, *10*, 2002260**
O-Co_2P-3	1.0 M KOH	160	*Adv. Mater.* **2017**, *29*, 1606980
mC-Mo-750	1.0 M KOH	145	*Adv. Funct. Mater.* **2018**, *30*, 1807419 .
Ni_2P/Ni	1.0M KOH	106	*ACS Appl. Mater.& Inter.* **2015**,*7*,2376
Ni-Se-Mo	1.0 M KOH	101	*Int. J. of Hydrogen Energ.* **2020**, *45*, 6015
N doped MoS_2	1.0 M KOH	141	*ChemElectroChem* **2020**, *7*, 336
MoS_2/$MoSe_2$	1.0 M KOH	235	*Nanoscale*, **2019**, *11*, 717
Ni-N-C	1.0 M KOH	147	*Energy Environ. Sci.***2019**,*12,*149
FeNiSe-NS/EG	1.0 M KOH	187	*Nanoscale*, **2019**, *11*,17571

Table S3 the Rs, Rct and CPE-P and CPE-T value of N-Mo_2C/NF, Mo_2C/NF, Mo_2N/NF and Pt/C for HER.

Catalyst	**R_S**	**R_{ct}**	**CPE-P**	**CPE-T**
N-Mo_2C/NF	1.791	27.95	0.819	0.001
Mo_2C/NF	1.944	36.30	0.857	0.001
Mo_2N/NF	1.393	62.42	0.830	0.008
Pt/C	1.914	6.725	0.810	0.143

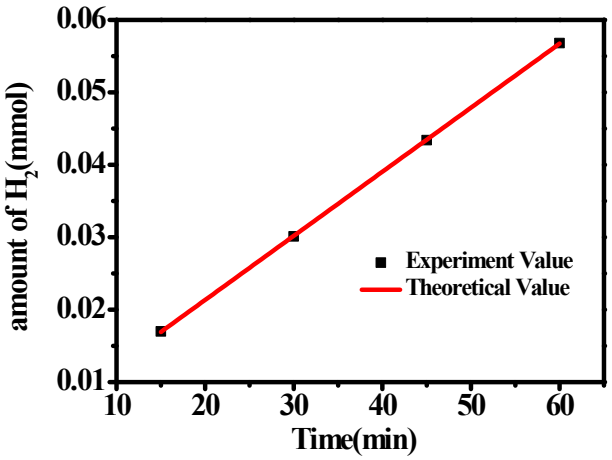

Figure S9. Theoretical and experimental tested H_2 evolution on N-Mo_2C/NF

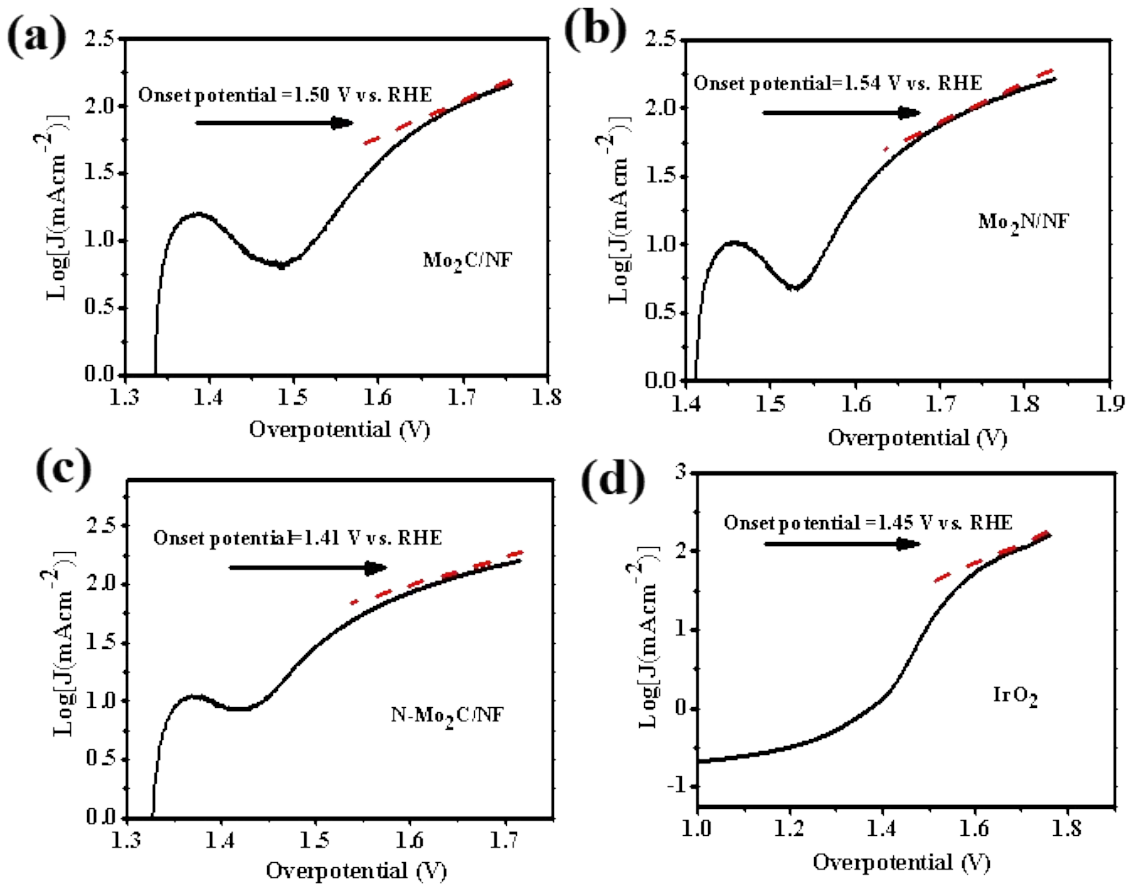

Figure S10. The plots of overpotential vs. log[J/(mA cm^{-2})] for Mo_2C/NF (a), Mo_2N/NF (b) and N-Mo_2C/NF (c), and IrO_2 (d) respectively.

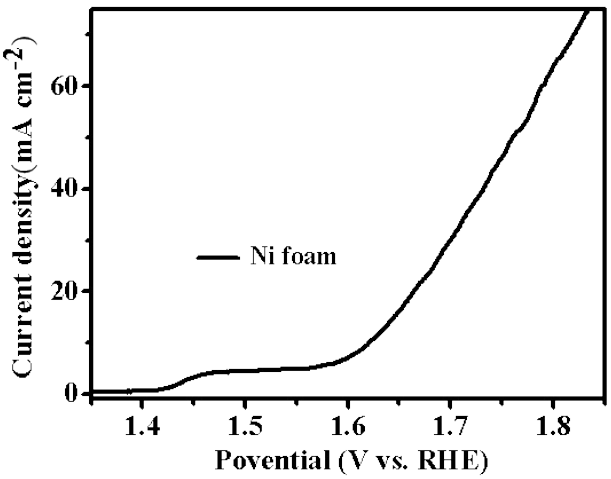

Figure S11. Polarzation curves of Ni foam in 1.0 M KOH at scan of 5 mV s^{-1} for OER.

Table S4. OER performances of N-Mo_2C/NF and other electrocatalysts reported in previously literatures.

Catalyst	**Media**	**(mV) at j=10mA cm^{-2}**	**Reference**
N-Mo_2C/NF	1.0 M KOH	230	This work
MoS_2-Ni	1.0 M KOH	280	*Small*, **2016**,*12*, 2975.
Ni–Ni_3S_2/NF	1.0 M KOH	310	*Nano Converg.* **2017**, *4*, 7.
Ni–Fe–Sn	1.0 M KOH	253	*Electrochimica Acta*, **2019**, *301*, 39
Co_3O_4/$NiCo_2O_4$/NF	1.0M KOH	270	*ACS Sustain. Chem. Eng*. **2019**, *7*,12214
ACo_2O_4 /NF	1.0 M KOH	271	*Int. J. of Hydrogen Energ.* **2018**, *43*,14360
Co-P film	1.0 M KOH	345	*Angew. Chem., Int. Ed.* **2015**, *54*, 6251
NiSSe/NF	1.0 M KOH	247	*Int. J. of Energ. Res.* **2019**, *44*,11
Ni_2P/NF	1.0 M KOH	290	*Energy Environ. Sci.* **2015**, *8*, 2347
CompactMoO_2/NF	1.0 M KOH	330	*Adv. Mater.* **2016**, *28*, 3785

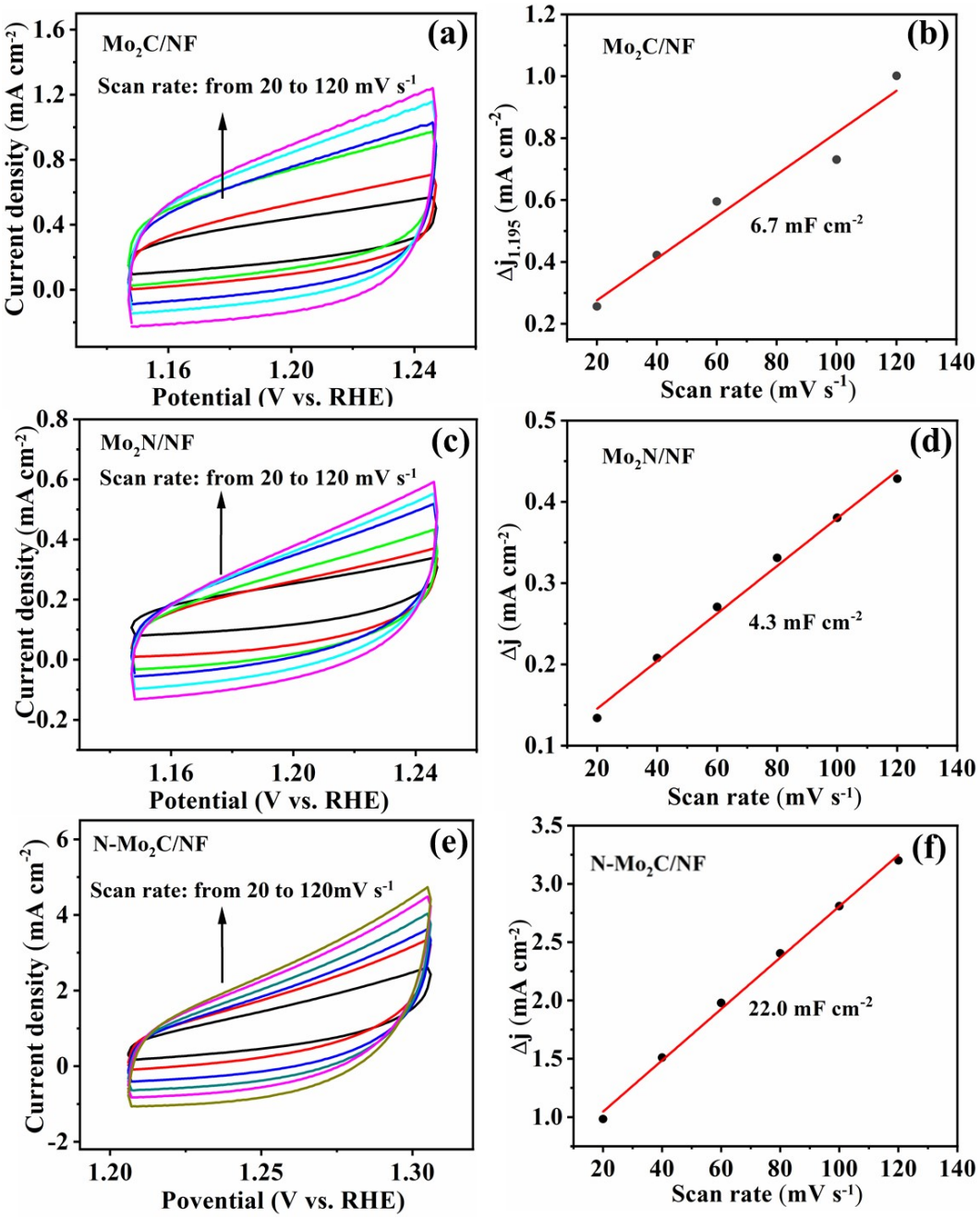

Figure S12. CV curves at different scan rates for (a) Mo_2C/NF, (c) Mo_2N/NF and (e) N-Mo_2C/NF. (b, d, f) Capacitive $i = i_a - i_c$ at the potential of 1.275 V vs. RHE plotted against scan rate fitted to estimate the electrochemical double-layer capacitances (C_{dl}).

Table 5 the Rs, Rct and CPE-P and CPE-T value of N-Mo_2C/NF, Mo_2C/NF, Mo_2N/NF and Pt/C for OER.

Catalyst	**R_S**	**R_{ct}**	**CPE-P**	**CPE-T**
N-Mo_2C/NF	1.614	4.39	0.546	0.169
Mo_2C/NF	1.754	15.40	0.831	0.002
Mo_2N/NF	2.164	14.15	0.541	0.499
IrO_2	1.776	8.10	0.749	0.001

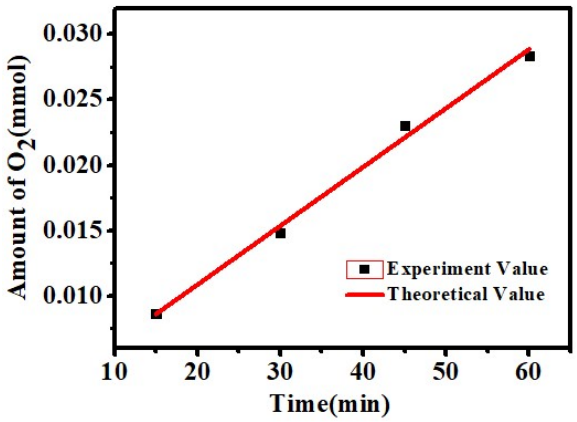

Figure S13. Theoretical and experimental tested O_2 evolution on N-Mo_2C/NF.

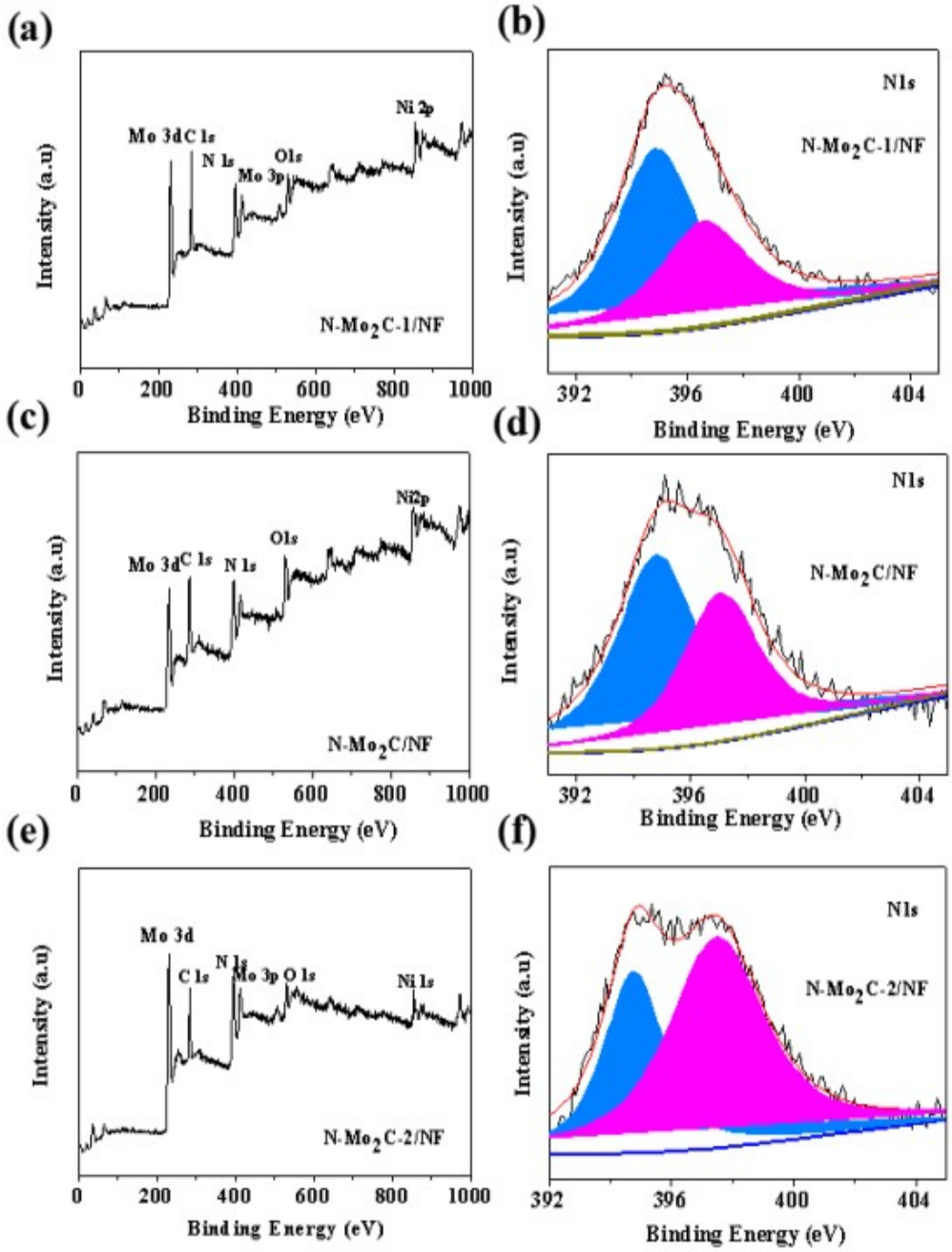

Figure S14. Full spectrum X-ray photoelectron spectroscopy (XPS) spectra of (a) N-Mo_2C-1/NF, (c) N-Mo_2C/NF and (e) N-Mo_2C-3/NF. N 1s XPS spectra of (b) N-Mo_2C-1/NF, (d) N-Mo_2C/NF and (f) N-Mo_2C/NF-3.

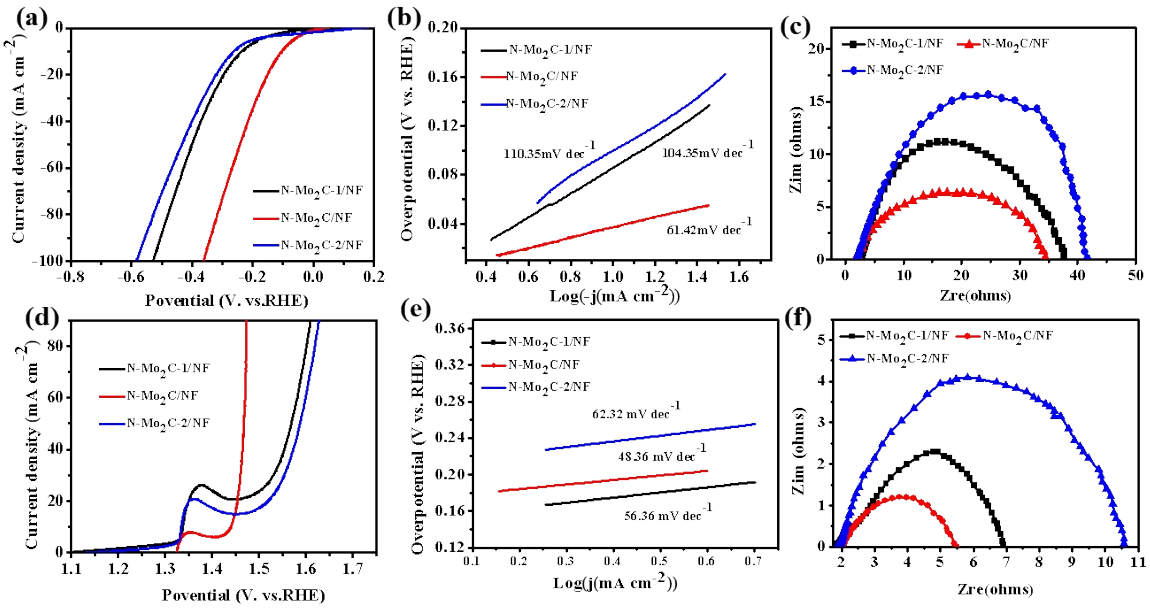

Figure S15. HER electrocatalytic performance. (a) Polarzation curves of N-Mo_2C-1/NF, N-Mo_2C/NF and N-Mo_2C-2/NF in 1.0 M KOH at scan of 5 mV s^{-1}. (b) Corresponding Tafel plots. (c) Nyquist plots obtained at 200 mV overpotential. OER electrocatalytic performance. (d) Polarzation curves of N-Mo_2C-1/NF, N-Mo_2C/NF and N-Mo_2C-2/NF in 1.0 M KOH at scan of 5 mV s^{-1}. (e) Corresponding Tafel plots and f) Nyquist plots.

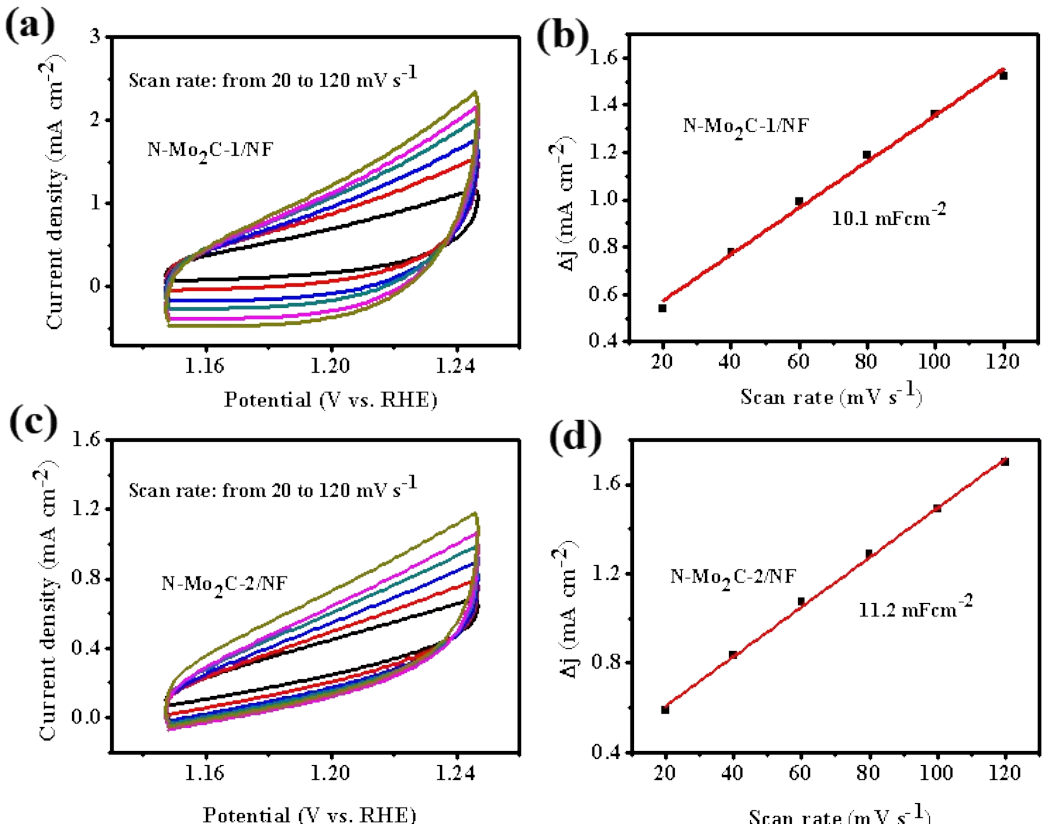

Figure S16. CV curves at different scan rates for (a) N-Mo_2C-1/NF and (c) N- Mo_2C-2/NF. (b, d) Capacitive i =i_a -i_c at the potential of 1.275 V vs. RHE plotted against scan rate fitted to estimate the electrochemical double-layer capacitances (C_{dl}).

Table S6. Comparison of two electrode water splitting cell voltage of N-Mo_2C/NF electrocatalyst with other nonprecious bifunctional electrocatalyst in 1 M KOH.

Catalysts	**Support**	**Overallvoltage @-10 mA cm^{-2}**	**Reference**
N-doped Mo_2C/NF-12	Ni foam	1.54V	This work
$NiCo_2S_4$ NW	Ni foam	1.63 V	*Adv. Funct. Mater*. **2016**,*26*, 4661
NiSe nanowire film	Ni foam	1.63 V	*Angew. Chem. Int. Ed.* **2015**, *54*, 9351
NiS/Ni foam	Ni foam	1.64 V	*Chem. Commun*. **2016**. *52*,1486
Ni_3S_2 Nanosheet Arrays	Ni foam	1.70 V	*J. Am. Chem.Soc.* **2015**, *137*, 14023
NiCoP nanowire array	Ni foam	1.64 V	*J. Mater. Chem. A* **2017**, *5*, 14828.
Ni-Fe-O nanowires	Ni foam	1.64 V	*Adv. Energy Mater.* **2017**, *8*, 1701347
Fe–MoS_2/Ni_3S_2/NF-2	Ni foam	1.61 V	*Dalton Transactions*, **2019**, *48*. 12186
NS-MnO_2	Ni foam	1.61 V	*Adv. Energy Mater.* **2017**, *7*, 1700005
Co-P films	Cu foam	1.64 V	*Angew. Chem.* **2015**, *127*, 6349

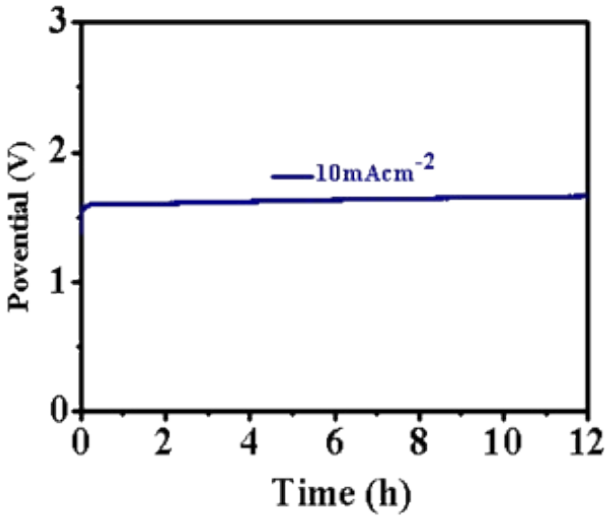

Figure S17. Long-term durability of N-Mo_2C/NF overall water splitting at a current density of 10 mA cm^{-2}.

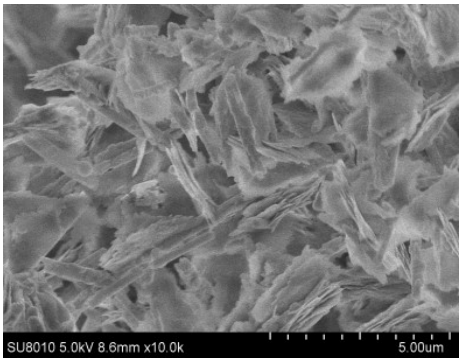

Figure S18. SEM image of N-Mo_2C/NF after overall water splitting reaction.

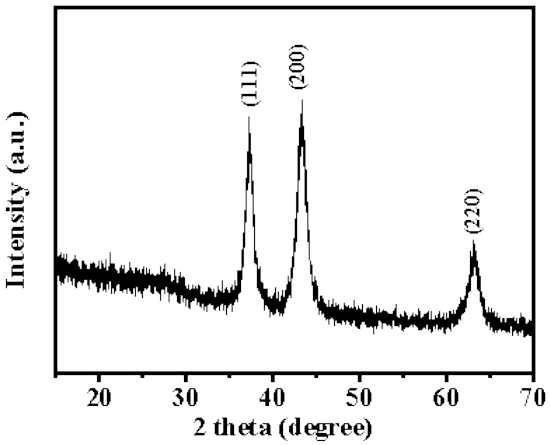

Figure S19. XRD of N-Mo_2C after overall water splitting reaction.

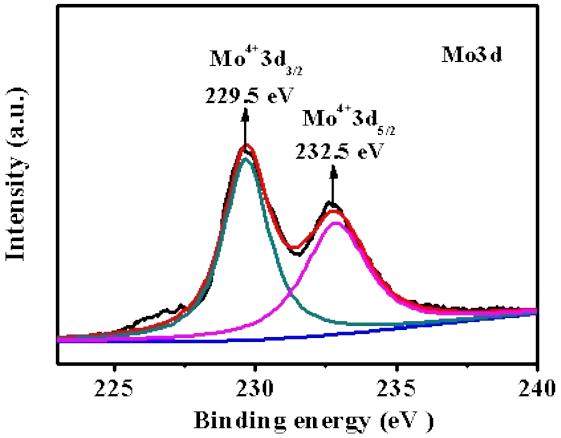

Figure S20. XPS spectra of Mo3d for N-Mo_2C/NF after overall water splitting reaction.

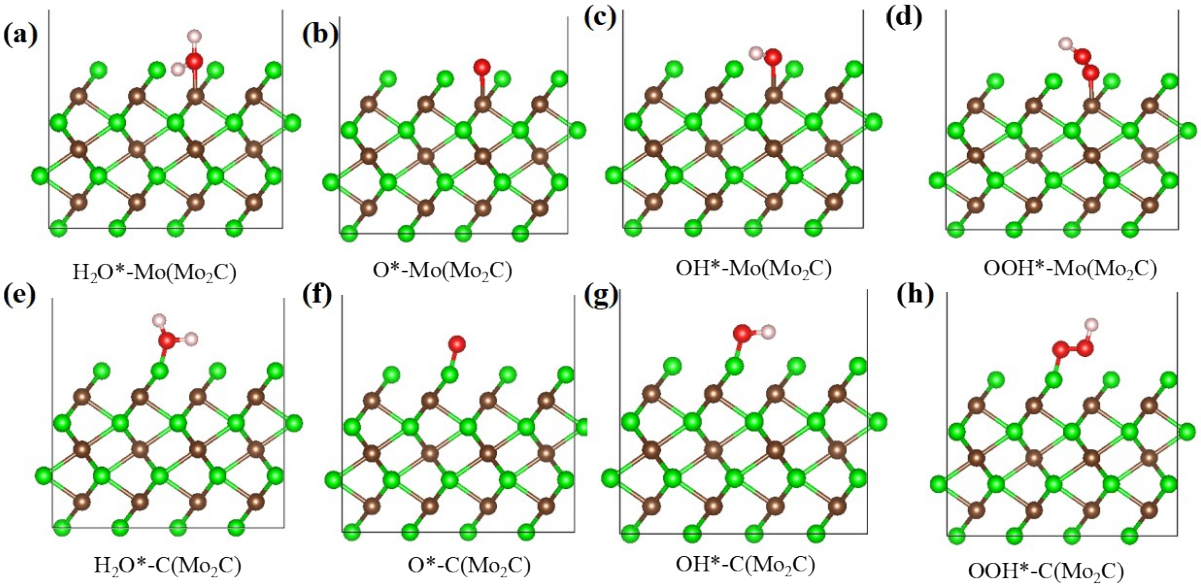

Figure S21. Chemisorption models of H_2O*, O*, OH* and OOH* intermediates on the surfaces of Mo_2C respectively

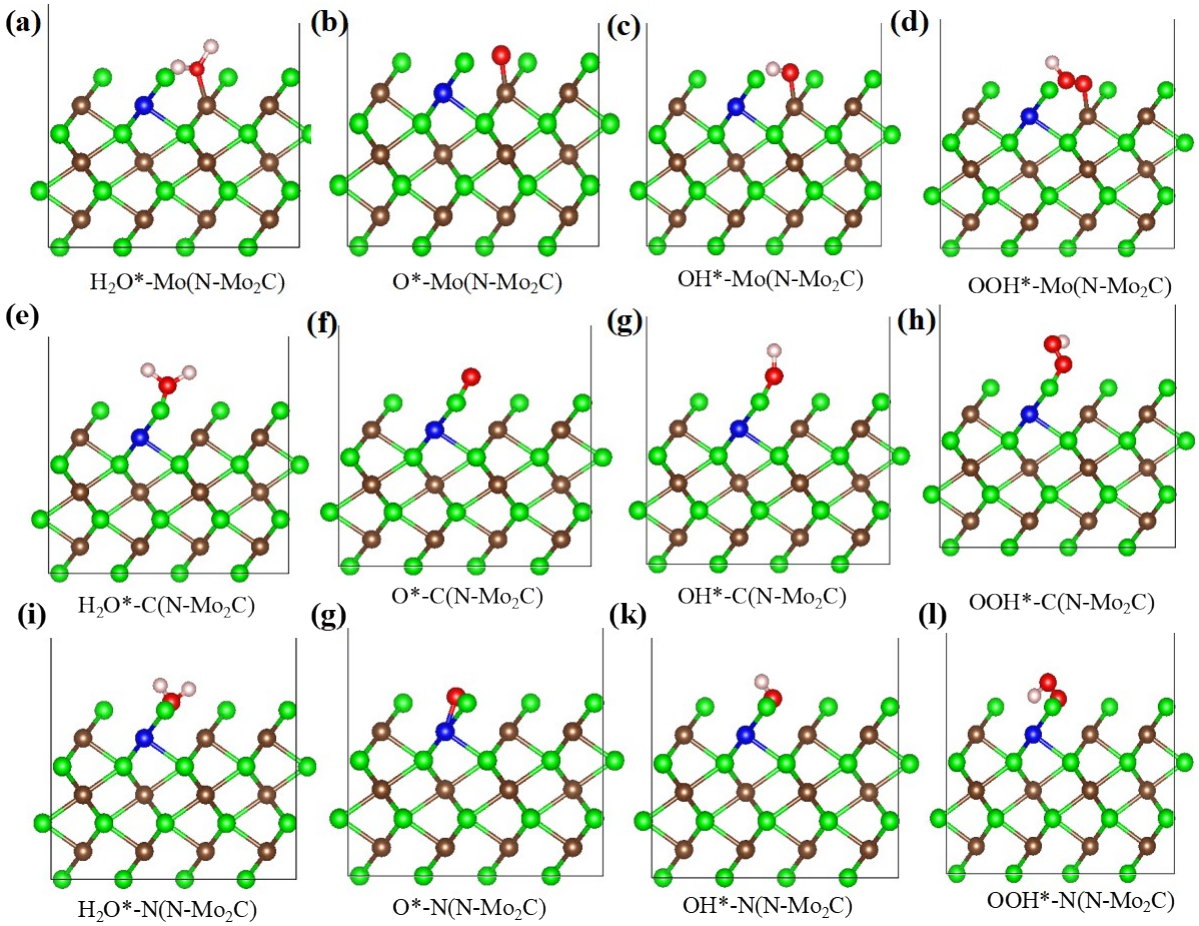

Figure S22. Chemisorption models of H_2O*, O*, OH* and OOH* intermediates on the surfaces of N-Mo_2C respectively

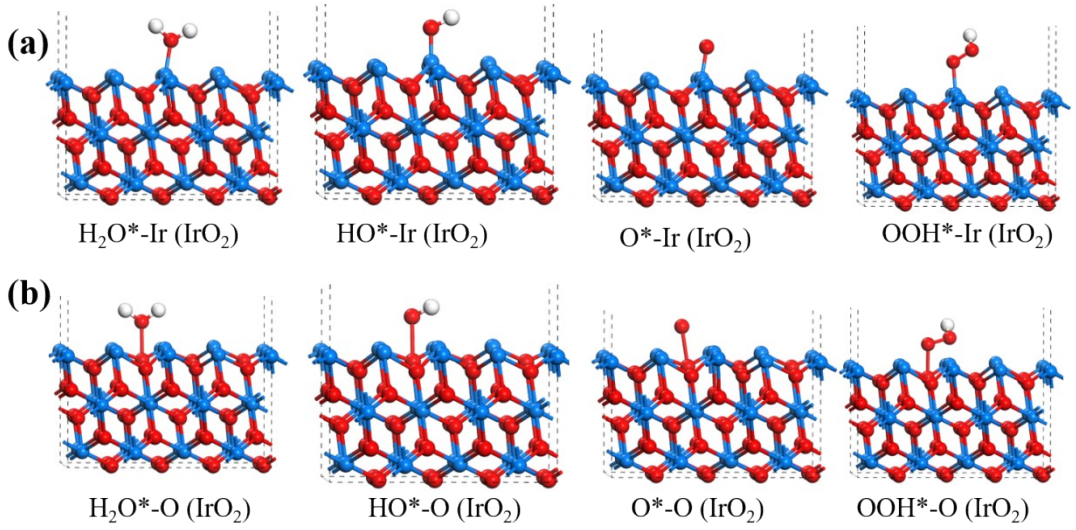

Figure S23. Chemisorption models of H_2O*, OH*, O*, and OOH* intermediates on the surfaces of N-Mo_2C respectively.

Table S7. Reaction (free) energy on the Mo_2C, N-Mo_2C and IrO_2

Catalyst	$H_2O(l) \rightarrow OH^*$	$OH^* \rightarrow O^*$	$O^* \rightarrow OOH^*$	$OOH^* \rightarrow O_2$
C-active site Mo_2C	1.21	0.85	1.69	1.17
Mo-active site Mo_2C	0.82	1.01	1.56	1.53
C-active site N-Mo_2C	1.05	0.96	1.62	1.29
Mo-active site N-Mo_2C	0.62	1.36	1.45	1.49
N-active site N-Mo_2C	0.76	1.18	1.58	1.40
Ir-active site IrO_2	0.70	1.30	1.46	1.46

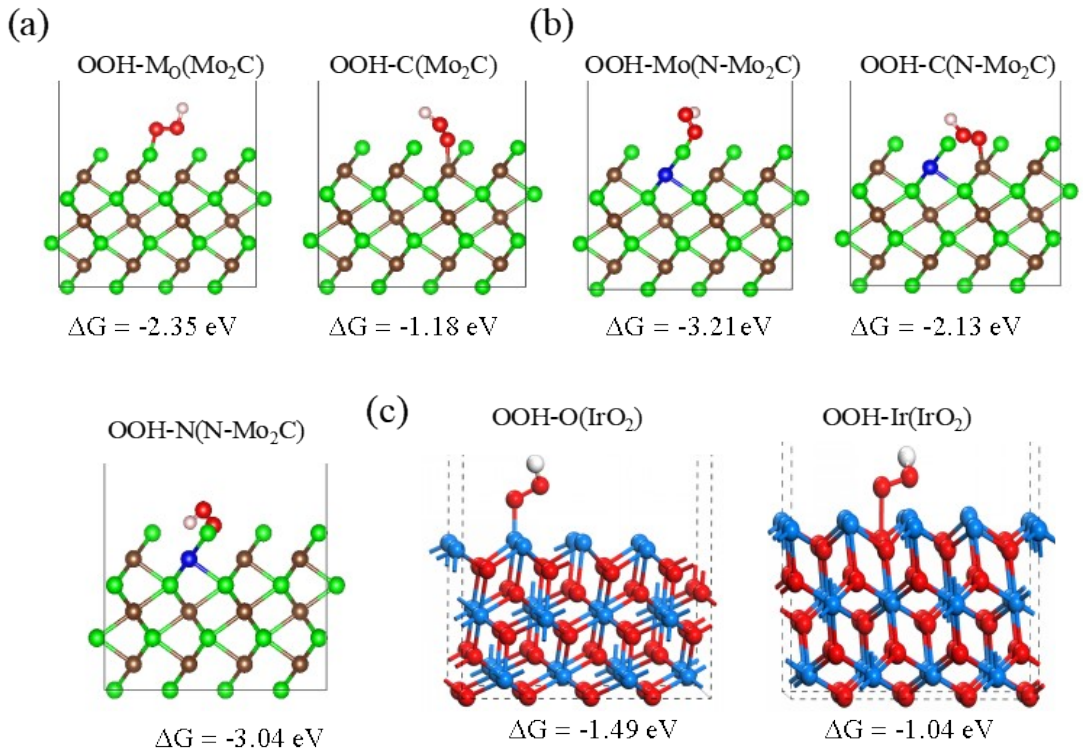

Figure S24. Chemisorption models of OOH* on the surfaces of Mo_2C, N-Mo_2C,and IrO_2 respectively.

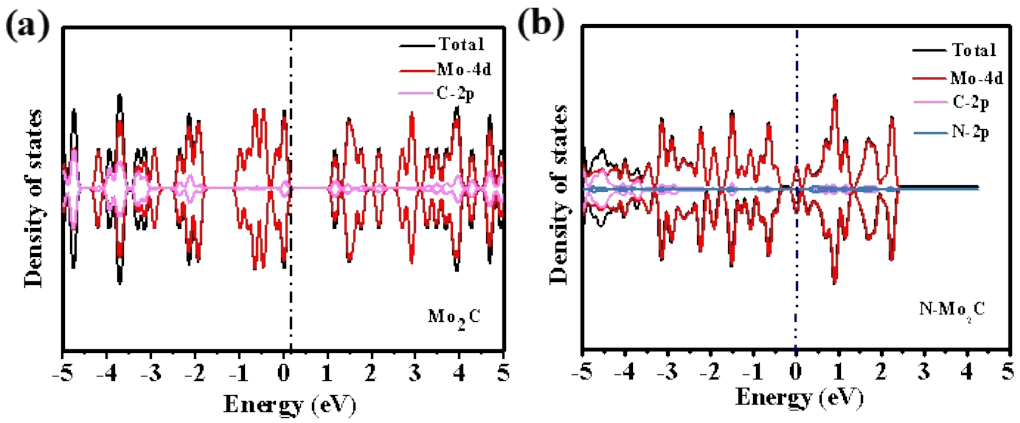

Figure S25. Density of state for Mo_2C and N-Mo_2C.

References

[1] a) L. Feng, A. Li, Y. Li, J. Liu, L. Wang, L. Huang, Y. Wang, X. Ge, *ChemPlusChem* **2017**, *82*, 483; b) H. Liu, X. Peng, X. Liu, G. Qi, J. Luo, *ChemSusChem* **2019**, *12*, 1334.

[2] X. Sun, Q. Shao, Y. Pi, J. Guo, X. Huang, *J. Mater. Chem. A* **2017**, *5*, 7769.

[3] Y. Chen, Z. Ren, H. Fu, X. Zhang, G. Tian, H. Fu, *Small*, **2018**, 1800763

[4] G. Kresse, J. Hafner, *Phys. Rev. B* **1994**, *49*, 14251; b) C. Zhu, A. L. Wang, W. Xiao, D. Chao, X. Zhang, N. H. Tiep, S. Chen, J. Kang, X. Wang, J. Ding, J. Wang, H. Zhang, H. J. Fan, *Adv. Mater.* **2018**, *30*, 170551.